Semihard Iron-Based Permanent-Magnet Materials

Li Yin[1,*] Rinkle Juneja,[1] Lucas Lindsay,[1] Tribhuwan Pandey[2] and David S. Parker[1]

[1]*Material Science and Technology Division, Oak Ridge National Laboratory, Oak Ridge, Tennessee 37831, USA*

[2]*Department of Physics, University of Antwerp, B2020, Antwerp, Belgium*

Permanent magnets generally require a favorable, but difficult-to-achieve combination of high magnetization, Curie point, and magnetic anisotropy. Thus there have been few, if any, viable permanent magnets developed since the 1982 discovery of $Nd_2Fe_{14}B$ [M. Sagawa, S. Fujimura, H. Yamamoto, Y. Matsuura, and S. Hirosawa, J. Appl. Phys. 57, 4094 (1985)]. Here we point out, both by direct first-principles calculations on the iron carbides and silicides Fe_5C_2, Fe_5SiC, and Fe_7C_3 as well as a discussion of recent experimental findings, that there are numerous rare-earth-free iron-rich potential permanent-magnet materials with sufficient intrinsic magnetic properties to reasonably achieve room-temperature energy products of 20–25 MG Oe. This is substantially better than the performance of the best available rare-earth-free magnets based on ferrite, as well as shape-anisotropy-employing alnico. These magnets could plausibly fill, at low cost, the present performance "gap" [J. M. D. Coey, Scr. Mater. 67, 524 (2012)] between the best rare-earth-free magnets and rare-earth magnets such as $Nd_2Fe_{14}B$ and Sm-Co.

I. INTRODUCTION

Permanent magnets [1,2] have been continuously studied for several decades due to their critical applications in modern technologies, such as typical memory devices [3], rapidly developing electric vehicles [4], wind turbines, and biomedical imaging [5,6]. To date, the permanent magnets have been mainly divided into two types [1,2]: one is the $Nd_2Fe_{14}B$ and Sm-Co rare-earth magnet category, while the other is the ferrite magnet, with alnico magnets occupying an intermediate regime. While rare-earth permanent magnets show high performance, they are generally of high price and limited availability. In comparison with the rare-earth permanent magnets, the ferrite magnets are lower cost but have correspondingly lower performance. Although some rare-earth-free permanent magnets have been reported, high-performance magnets among those materials generally contain the expensive heavy element Pt [2,7], which precludes the widespread use. Developing a low-cost "gap" permanent magnet between Nd-Fe-B and ferrite magnets is therefore urgent for technology.

Iron-silicon and iron-carbon compounds and alloys are ubiquitous in the making of steel and other iron-based compounds. Cementite, or Fe_3C, commonly forms in the blast furnaces within which steel is made, along with other compounds in this category such as Fe_2C, the Hägg carbide Fe_5C_2, and the relatively unknown Fe_7C_3. Hägg

carbide Fe_5C_2 was produced as a by-product of the Fisher-Tropsch reaction during the synthesis of gasoline [8]. Similarly, silicon is often used in steel as the precipitates whose formation it aids significantly strengthen it. Despite their substantial presence in perhaps the most common industrial material in societal usage today, it is only recently [9] that the thermodynamics, including stability, of these secondary phases has been studied in detail.

In this context it is perhaps unsurprising that these compounds have undergone relatively little study for applications other than structural materials, despite the fact that the (ferro)magnetism of iron itself has been known since antiquity and all the compounds listed above are known to be ferromagnetic. Since iron, carbon, and silicon are all inexpensive, abundant elements, this immediately suggests the possibility of inexpensive "gap" [1] permanent magnets based on these compounds. One complicating factor, however, as found in Ref. [9] is that several of these materials are thermodynamically metastable at $T = 0$ and zero pressure, so that their laboratory synthesis has generally proved problematic. Nevertheless, since a permanent magnet itself is a metastable configuration, consisting of grains carefully engineered to avoid the bulk magnetization-destroying formation of domains, one ought not consider the metastability of these bulk phases as a prohibition on their usage in permanent-magnet applications. As with permanent magnet magnetization, it should be possible to find experimental means of "freezing in" the metastable composition. One means of achieving this might be via small amounts of manganese substitution, as Materials Project

————
*yinl@ornl.gov

calculations find the manganese compounds Mn_5SiC and Mn_5C_2 to be significantly more thermodynamically stable than their iron-based counterparts. In addition, the magnetization in Mn_5SiC [10] is not saturated even at an applied magnetic field of 2.6 T, which is some $3\times$ larger than our estimated anisotropy field of 0.8 T for Fe_5SiC. This suggests that Mn substitution into Fe_5SiC probably increases the anisotropy fields.

So far, many synthesis methods have been utilized for iron-carbide and iron-silicocarbide compounds. The pure phase of Hägg carbide Fe_5C_2 nanoparticle with a spherical size of 100 nm can be *in situ* synthesized via a chemical-solution route, using amorphous Fe nanoparticles as iron feedstock and Oleylamine as carbon feedstock [11]. The iron silicocarbide Fe_5SiC was synthesized by mechanical alloying [12–14]. Solvothermal synthesis of Fe_7C_3 nanostructure has been achieved with phase and morphology control [15]. Orthorhombic Fe_7C_3 was synthesized in a multianvil press [16,17]. The various and rapidly developing synthesis methods provide the foundation for future application of these iron-carbide and iron-silicocarbide compounds. The first-principles calculations presented here suggest that one of the materials reported in the literature, Fe_5SiC, may in fact show sufficient "intrinsic" properties to yield good permanent magnet performance. Note that these "intrinsic" properties are generally comprised of large values of the saturation magnetization M_s, the Curie point T_c, and the first magnetic anisotropy constant K_1 (for a uniaxial material).

Of relevance for the following discussion is that both materials exhibit a relatively unusual stoichiometry, and related to this exhibit complex monoclinic structures, with nonorthogonal axes. While most high-performance magnets, such as $Nd_2Fe_{14}B$, $SmCo_5$, and the ferrites, form in a two-dimensional structure with uniaxial anisotropy, there is no *a priori* requirement for a two-dimensional (as opposed to a three-dimensional) structure for high-performance magnet properties. Indeed, recent work by one of us on orthorhombic HfMnP [18] finds a substantial magnetic anisotropy in this material.

The main magnetic anisotropy requirement for a permanent magnet is in fact a significant anisotropy from the easy axis relative to each of the principal axis directions, which imposes no explicit requirement for two dimensionality on the material. In practice, this requirement is approximately as restrictive for three-dimensional materials (in terms of the probability that a randomly chosen ferromagnet has desirable anisotropy properties), cubic materials of course excepted, as for two-dimensional materials.

Typically for a high-performance magnet with coercivity at least as large as the magnetization, one requires the "magnetic hardness parameter" $\kappa = \sqrt{K_1/(\mu_0 M_s^2)} > 1$ [19], where K_1 is the magnetocrystalline energetic difference (on a volumetric basis) of the two easiest principal directions, M_s the saturation magnetization, and μ_0 the

vacuum permeability. While neither of the materials studied here has this level of anisotropy, the anisotropy is sufficient that a comparatively low-cost (considering the abundance of Fe, Si, and C) "gap" magnet with 20–25 MG Oe energy product magnet is possible based on these materials. As Coey has written [1], such a magnet would substantially benefit the technological sector, given that $Nd_2Fe_{14}B$ is frequently used in applications where a less powerful, less costly (but presently nonexistent) magnet would suffice. Indeed, Ref. [12] has already found a significant coercivity of 0.4 kOe in Fe_5SiC despite a near-complete lack of the processing optimization usually necessary for significant energy products. Note that an energy product as high as 6 MG Oe, based on these parameters is possible even in this relatively unoptimized state. It is therefore plausible that significantly larger energy products can be achieved in these materials, for appropriate processing conditions.

In this work, we study the magnetic properties of Fe_5C_2, Fe_5SiC, and hexagonal and orthorhombic Fe_7C_3 from first principles. Among the studied compounds, we find a technologically relevant magnetic anisotropy of 0.44 MJ/m³ and hardness parameter κ of 0.50 in Fe_5SiC, along with the substantial magnetization exceeding 1.4 T and a high Curie point above 788 K. These magnetic properties make Fe_5SiC a promising candidate for rare-earth-free and low-cost permanent magnets, which pave a way for "gap" permanent magnets. Following our first-principles results, we present a discussion of the feasibility of producing such low-anisotropy "gap" magnets from several Fe-based materials, including those studied here. We end with a conclusion.

II. CALCULATION METHODS

The calculations are performed by using the all-electron-density functional code WIEN2k [20,21] with the generalized-gradient approximation of Perdew, Burke, and Ernzerhof [22]. The linearized augmented plane-wave (LAPW) method [23] is employed in all of the calculations. The RK_{max} [product of the smallest LAPW sphere radius (R) and the interstitial plane-wave cutoff (K_{max})] of 7.0 is used for good convergence. The lattice constants of Fe_5C_2 [24,25], Fe_5SiC [12], hexagonal Fe_7C_3 [26], and orthorhombic Fe_7C_3 [16,17,27] are fixed to their experimental values, which are displayed in Table I and Fig. 1. The internal atomic coordinates are relaxed until forces on all the atoms are less than 1 mRy/bohr. For the structure relaxation, 1000 **k** points are used in the full Brillouin zone. The magnetic anisotropy energy (MAE) is calculated with spin-orbit coupling, based on the assumed collinear spin arrangement. The charge convergence criteria is set to be 0.0001 e. MAE_{a2-a1} is defined as $(E_{a2} - E_{a1})/V$. E_{a2} and E_{a1} are the total energies of the system for the magnetization oriented along the $a2$ and $a1$ directions,

TABLE I. Lattice constants, unit-cell volumes, total magnetic moment (m_{tot}), atomic spin moments (μ_{Fe}, μ_{Si}, and μ_C), bulk modulus (B), shear modulus (G), and Pugh's ratio (G/B) in relaxed Fe_5C_2, Fe_5SiC, hexagonal (-h) and orthorhombic (-o) Fe_7C_3.

Compound	Fe_5C_2	Fe_5SiC	$Fe_7C_3 - h$	$Fe_7C_3 - o$
a (Å)	11.57	10.04	6.88	11.98
b (Å)	5.06	7.94	6.88	4.52
c (Å)	4.57	7.47	4.54	13.77
α (°)	90.00	90.00	90.00	90.00
β (°)	90.00	90.00	90.00	90.00
γ (°)	82.27	90.00	120.00	90.00
Volume (Å^3)	132.56	297.94	186.22	745.25
m_{tot} (μ_B/f.u.)	8.93	9.56	12.14	12.56
μ_{Fe} (μ_B)	1.75	2.02	1.80	1.82
μ_{Si} (μ_B)	–	−0.08	–	–
μ_C (μ_B)	−0.10	−0.11	−0.10	−0.11
κ	0.36	0.50	0.37	0.33
B (GPa)	199.9	188.7	216.7	224.6
G (GPa)	83.4	51.9	86.2	85.0
G/B	0.4	0.3	0.4	0.4

The hardness parameter κ between easy and next-easiest axes is listed for these Fe-based compounds.

FIG. 1. Geometry of (a) Fe_5C_2, (b) Fe_5SiC, (c) hexagonal (-h) and (d) orthorhombic (-o) Fe_7C_3. The dotted circle, solid circle, and solid hexagon in the coordinated axes from (a)–(d) denote the easy, next-easiest, and hard axes in corresponding iron-carbide and iron-silicocarbide compounds.

respectively. V indicates the volume of the primitive cell. Herewith, [100], [010], and [001] directions are considered in all the iron-carbide and iron-silicocarbide compounds to analyze their axial anisotropy. As mentioned above, the magnetic hardness parameters in these compounds are calculated as $\kappa = \sqrt{K_1/(\mu_0 M_s^2)}$ [1,7,19], where K_1 indicates the magnetocrystalline anisotropy energy (i.e., the calculated MAE in this work), M_s denotes the saturation magnetization. μ_0 is the vacuum permeability, which is defined as $4\pi \times 10^{-7}$ T m/A.

The formation energies of Fe_5C_2, Fe_5SiC, hexagonal and orthorhombic Fe_7C_3 are calculated in the Vienna *ab initio* simulation package [28,29]. The projector augment wave pseudopotentials and generalized-gradient approximation are employed in the calculations [30,31]. The plane-wave energy cutoff is 400 eV. The Brillouin zone is sampled with Γ centered $2 \times 4 \times 4$, $2 \times 3 \times 3$, $2 \times 2 \times 3$, and $2 \times 5 \times 2$ k-point meshes for Fe_5C_2, Fe_5SiC, hexagonal and orthorhombic Fe_7C_3, respectively. The convergence criteria for energy and atomic forces are set to 10^{-6} eV and 0.001 eV/Å, respectively. In addition, the spin-polarized phonon dispersions are calculated for Fe_5C_2, Fe_5SiC, hexagonal and orthorhombic Fe_7C_3. The $2 \times 2 \times 2$ supercell with 112 atoms, $2 \times 2 \times 2$ supercell with 224 atoms, $2 \times 2 \times 3$ supercell with 240 atoms, and $1 \times 3 \times 1$ supercell with 240 atoms are used for the phonon calculations in Fe_5C_2, Fe_5SiC, hexagonal and orthorhombic Fe_7C_3, respectively. The $2 \times 2 \times 2$, Γ only, $2 \times 2 \times 3$, and $1 \times 3 \times 1$ k meshes are used for the phonon calculations in Fe_5C_2, Fe_5SiC, hexagonal and orthorhombic
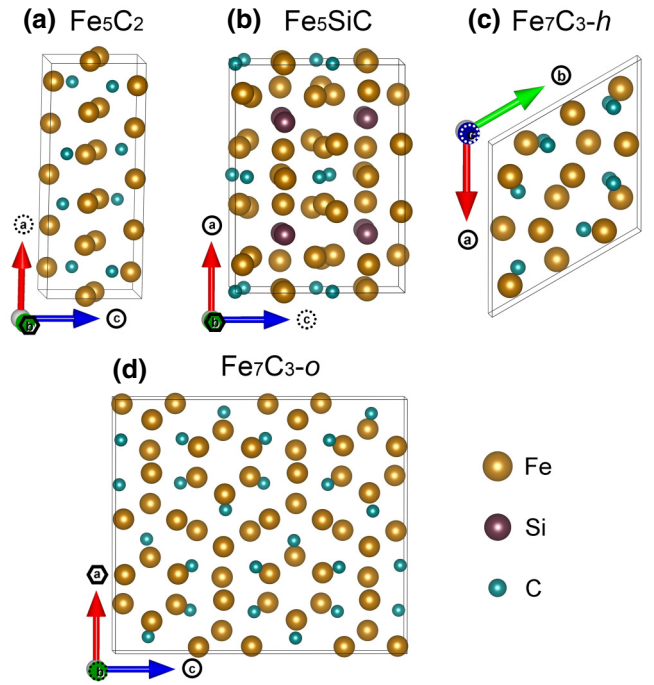
Fe_7C_3, respectively. The spin-polarized elastic constants of Fe_5C_2, Fe_5SiC, hexagonal and orthorhombic Fe_7C_3 are calculated with the stress-strain methodology, as implemented in the Vienna *ab initio* simulation package. In particular, a high-energy cutoff of 700 eV in Fe_5C_2, hexagonal Fe_7C_3, orthorhombic Fe_7C_3 and 500 eV in Fe_5SiC is used for calculating the elastic constants. The convergence criterion for energy is set to 10^{-8} eV for elastic calculations.

III. RESULTS

First of all, MAE is a small quantity of the order of meV, which depends sensitively on the number of k points used. In previous studies, the 1000, 1200, and 2600 k points in Fe-Co-C [32,33] and Fe-Si-B [34] compounds and 10 000 k points in ZrMnP (HfMnP) [18] compounds have been used for calculating MAE through WIEN2k. In this work, different k points are tested to calculate the MAE. In Fe_5C_2, the calculated MAE at different k points is shown in Fig. 2, where the varying trend of MAE$_{[010]-[100]}$ with k points is similar to the MAE$_{[001]-[100]}$ case. It can be found that the values of MAE in Fe_5C_2 are similar when the k points are larger than 2000. The difference in calculated MAE$_{[010]-[100]}$ at 3000 and 6000 k points is 0.49%, and the difference in calculated MAE$_{[001]-[100]}$ at 3000 and 6000 k points is 5.68%. The MAE results

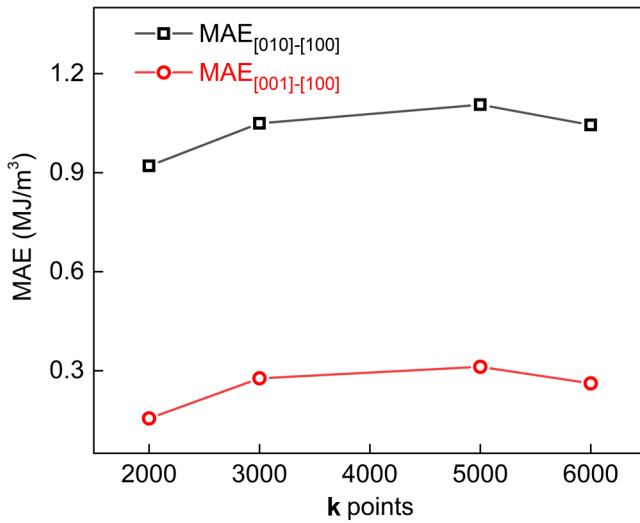FIG. 2.   Calculated $MAE_{[010]-[100]}$ and $MAE_{[001]-[100]}$ in Fe_5C_2 with different **k** points.

reported for Fe_5C_2 use 6000 **k** points. We further check the **k**-affected MAE in Fe_5SiC and orthorhombic Fe_7C_3. The difference in $MAE_{[100]-[001]}$ in Fe_5SiC at 2000 and 5000 **k** points is 1.96%. In orthorhombic Fe_7C_3, the difference in $MAE_{[100]-[010]}$ in Fe_5SiC at 2000 and 5000 **k** points is 0.92%. So, the MAE in Fe_5SiC and orthorhombic Fe_7C_3 are reported using the 2000 **k** points, which is also employed in hexagonal Fe_7C_3. Herewith, the iron-carbide and iron-silicocarbide compounds can be mainly represented by Fe_3C, Fe_4C, Fe_5C_2, Fe_7C_3, and Fe_5SiC. Among these, Fe_4C is in the cubic structure [35] and the magnetic anisotropy of orthorhombic Fe_3C is as low as 0.05 MJ/m^3 [36], which is substantially insufficient as a permanent

magnet. So, we analyze only the magnetic properties of Fe_5C_2, Fe_5SiC, and Fe_7C_3 in this work.

Hägg carbide Fe_5C_2 is in the space group of $C2/c$ with the monoclinic structure, whose lattice constants are listed in Table I. The easy and next-easiest axes of Fe_5C_2 lie in the [100] and [001] directions, as shown in Fig. 1(a). The hard axis is in the [010] direction. The MAE between the easy and hard axes in Fe_5C_2 is 1.04 MJ/m^3, which is rather significant for materials containing only relatively light elements such as Fe and C. It is, in fact, slightly larger as the value for hcp Co [37]. Moreover, as shown in Fig. 3(a), the $MAE_{[001]-[100]}$ between the easy and next-easiest axes in Fe_5C_2 is 0.26 MJ/m^3, which is low but likely sufficient for the energy products of 20–25 MG Oe. Meanwhile, the magnetization of Fe_5C_2 can be as large as 1.57 T, as shown in Fig. 3(b). The strong magnetization in Fe_5C_2 has created attention for biomedical applications [38], such as the tumor imaging. Here, we discuss whether the magnetization of 1.57 T in Fe_5C_2 is strong enough for a permanent magnet. Moreover, the Curie point of Fe_5C_2 is about 520 K [39], which is suitable in permanent magnets. So, the significant magnetic anisotropy, the strong magnetization, and a high Curie point make Fe_5C_2 a candidate for a permanent magnet, especially the 20–25 MG Oe energy product magnet.

Next, the magnetic properties of iron silicocarbide Fe_5SiC and iron carbide Fe_7C_3 are illustrated. Fe_5SiC shows the orthorhombic structure in the space group of $Cmc21$. In Fe_5SiC, the easy, next-easiest, and hard axes are in the [001], [100], and [010] directions, which produce a $MAE_{[100]-[001]}$ of 0.44 MJ/m^3 and the $MAE_{[010]-[001]}$ of 0.71 MJ/m^3. Moreover, the magnetization of Fe_5SiC is 1.49 T as shown in Fig. 3(b), and the Curie point of Fe_5SiC is, from experimental measurement, 788 K [12]. So, the significant uniaxial anisotropy, strong magnetization, and
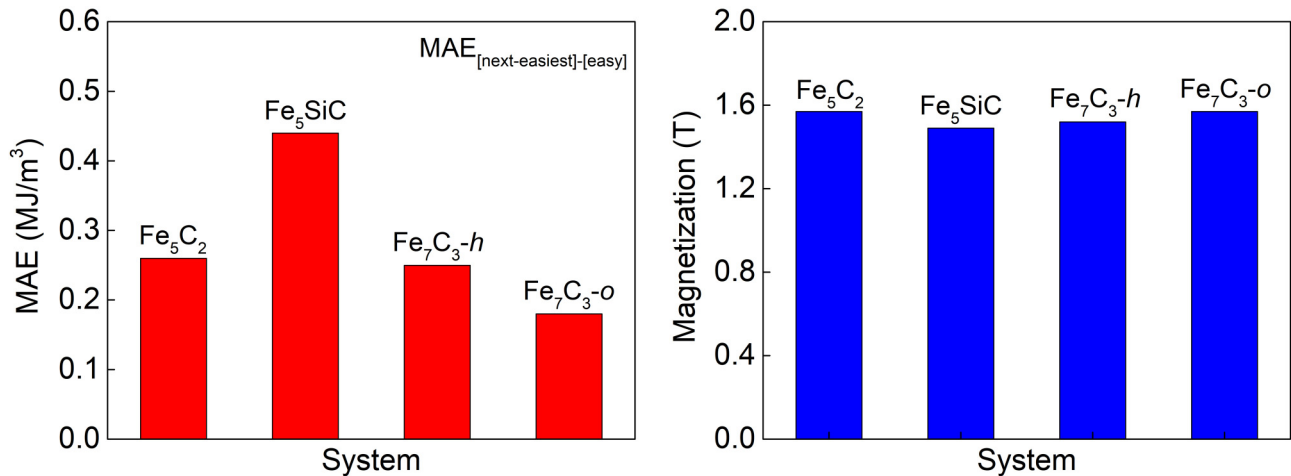

FIG. 3.   (a) MAE and (b) magnetization in Fe_5C_2, Fe_5SiC, hexagonal (-*h*) and orthorhombic (-*o*) Fe_7C_3, with GGA + SOC calculations. The MAE in (a) denotes the MAE between the easy and next-easiest axes in iron-carbide and iron-silicocarbide compounds, corresponding to the dotted and solid circles in Fig. 1.

high Curie point suggest that Fe_5SiC is a possible permanent magnet candidate. For Fe_7C_3, the hexagonal and orthorhombic phases are studied here. The hexagonal and orthorhombic Fe_7C_3 are in the space group of $P6_3mc$ and $Pbca$, respectively, whose lattice constants are listed in Table I. As shown in Fig. 3(b), the calculated magnetization in hexagonal or orthorhombic Fe_7C_3 is close to that in Fe_5C_2, which is consistent with the experimental results [11,15]. The Curie point of hexagonal Fe_7C_3 is 523 K [40,41], which is similar to that in Fe_5C_2. However, the hexagonal Fe_7C_3 shows a uniaxial magnetic anisotropy of 0.25 MJ/m^3, where the easy axis lies in the [001] direction. The orthorhombic Fe_7C_3 also shows the axial anisotropy, where the easy, next-easiest, and hard axes lie in the [010], [001], and [100] directions, respectively. In orthorhombic Fe_7C_3, the $MAE_{[100]-[010]}$ is 0.28 MJ/m^3, and the $MAE_{[001]-[010]}$ is 0.18 MJ/m^3. As shown in Fig. 3(a), the axial anisotropy in Fe_5C_2, hexagonal or orthorhombic Fe_7C_3 is obviously smaller than that in Fe_5SiC. Moreover, the hardness parameter κ of Fe_5SiC is also higher than the κ in Fe_5C_2 and Fe_7C_3, as listed in Table I. Finally, the relatively large axial anisotropy, considerable hardness parameter, strong magnetization, and a high Curie point make Fe_5SiC a promising candidate for permanent magnets without rare-earth or expensive contents.

We further analyze the total and atom-resolved density of states (DOS) for Fe_5C_2 and Fe_5SiC, as shown in Figs. 4 and 5. In both Fe_5C_2 and Fe_5SiC, the Fe atoms show strong hybridization with C atoms almost in the whole energy window, where the Fe and C atoms are mainly attributed to the d and p electrons, respectively. As compared with

FIG. 5. Total (dotted line) and atomic (solid lines) DOS in Fe_5SiC. The inset denotes the enlarged regions marked by the gray color for clarity. The positive and negative values in the vertical axis indicate the spin-up and spin-down channels, respectively. The Fermi level is 0 eV.

Fe_5C_2 (Fig. 4), the Fe_5SiC shows an extra intermediate state as the gray color marked in Fig. 5. In particular, the Si atoms in Fe_5SiC mainly occupy the energy window of the intermediate state, where the p electrons of Si still show strong hybridization with the Fe d electrons (see the inset of Fig. 5). As mentioned above, the magnetization of Fe_5C_2 or Fe_5SiC is about 1.5 T, which is comparable to the known ferromagnets with and without the critical rare-earth elements. The sufficient hybridization between Fe d and C p (Si p) orbits might provide foundations for the strong magnetization in Fe_5C_2 and Fe_5SiC.

In addition, we calculate the formation energy for these iron-carbide and iron-silicocarbide compounds. The system with a lower value of formation energy will be more stable at high temperatures. The formation energies E_f (compound) of Fe_5C_2, Fe_5SiC, hexagonal (-h) and orthorhombic (-o) Fe_7C_3, are calculated, on a per-atom basis, based on their elementary substances [Eq. (1)] and stable secondary phases [Eqs. (2) and (3)] as follows:

$$E_f(Fe_5C_2) = [E(Fe_5C_2) - 5E(Fe) - 2E(C)]/7,$$

$$E_f(Fe_5SiC) = [E(Fe_5SiC) - 5E(Fe) - E(Si) - E(C)]/7,$$

$$E_f(Fe_7C_3\text{-}h) = [E(Fe_7C_3\text{-}h) - 7E(Fe) - 3E(C)]/10,$$

$$E_f(Fe_7C_3\text{-}o) = [E(Fe_7C_3\text{-}o) - 7E(Fe) - 3E(C)]/10; \tag{1}$$

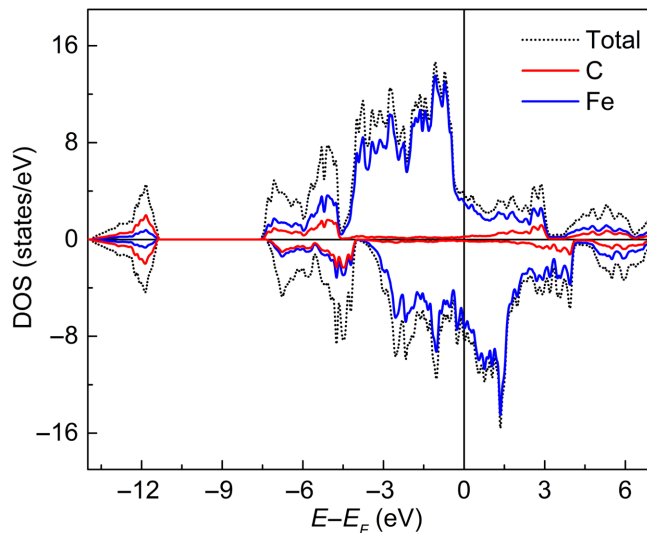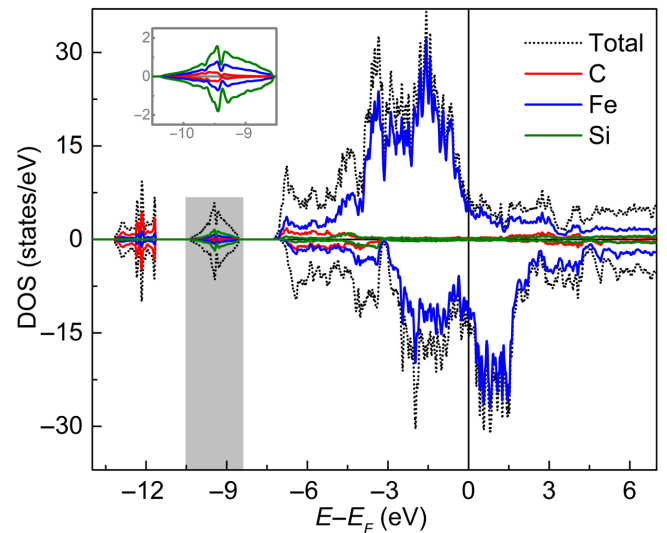$$E_f(Fe_5SiC) = [E(Fe_5SiC) - E(FeSi) - 4E(Fe) - E(C)]/7; \tag{2}$$

FIG. 4. Total (dotted line) and atomic (solid lines) DOS in Fe_5C_2. The positive and negative values in the vertical axis denote the spin-up and spin-down channels, respectively. The Fermi level is 0 eV.

$$E_f(\text{Fe}_5\text{SiC}) = [E(\text{Fe}_5\text{SiC}) - E(\text{SiC}) - 5E(\text{Fe})]/7. \quad (3)$$

The applied energies of each material correspond to their total energies. The Fe, Si, C, FeSi, and SiC energies are calculated from their stable phases [42]. The calculated elemental formation energies of Fe_5C_2, Fe_5SiC, hexagonal and orthorhombic Fe_7C_3 in Eq. (1) are 0.057, -0.158, 0.085, and 0.064 eV/atom, respectively. For Fe_5SiC, the calculated formation energies in Eqs. (2) and (3) are -0.011 eV/atom and -0.099 eV/atom, respectively. The formation energies of these compounds are lower than 90 meV/atom. It can be found that Fe_5SiC with the negative formation energy is thermally the most stable among these compounds. The positive formation energies of iron-carbide compounds show the trend of stability from high to low as $\text{Fe}_5\text{C}_2 >$ orthorhombic $\text{Fe}_7\text{C}_3 >$ hexagonal Fe_7C_3, which is consistent with previous studies [9]. Meanwhile, these compounds have been synthesized in experiments, and the synthesis has been controllable with the aid of various preparation methods [12,15,16,24], which should be very helpful for further utilization as permanent magnets.

IV. DISCUSSION

Considering these iron-carbide and iron-silicocarbide compounds are phases that crystallize in low-symmetry lattices, their mechanical properties should be investigated. We calculate the elastic constants of Fe_5C_2, Fe_5SiC, hexagonal and orthorhombic Fe_7C_3 compounds. The mechanical stability is assessed by checking the necessary and sufficient conditions to be satisfied by the elastic constants [43]. The elastic constants values for all the compounds are presented in the Voigt notation. In Fe_5C_2, the elastic tensor is

$$C = \begin{pmatrix} 318.9 & 150.4 & 127.3 & 0.0 & -0.3 & 0.0 \\ 150.4 & 296.9 & 132.8 & 0.0 & 20.0 & 0.0 \\ 127.3 & 132.8 & 366.8 & 0.0 & -0.5 & 0.0 \\ 0.0 & 0.0 & 0.0 & 130.5 & 0.0 & -10.1 \\ -0.3 & 20.0 & -0.5 & 0.0 & 124.1 & 0.0 \\ 0.0 & 0.0 & 0.0 & -10.1 & 0.0 & 31.9 \end{pmatrix}.$$

The six eigenvalues of the above matrix are 602.4, 225.0, 162.2, 131.5, 117.2, and 30.9, satisfying the elastic stability criteria that all eigenvalues of C must be positive. In Fe_5SiC, the elastic tensor is

$$C = \begin{pmatrix} 311.3 & 128.4 & 131.8 & 0.0 & 0.0 & 0.0 \\ 128.4 & 269.2 & 139.1 & 0.0 & 0.0 & 0.0 \\ 131.8 & 139.1 & 324.6 & 0.0 & 0.0 & 0.0 \\ 0.0 & 0.0 & 0.0 & 6.3 & 0.0 & 0.0 \\ 0.0 & 0.0 & 0.0 & 0.0 & 112.6 & 0.0 \\ 0.0 & 0.0 & 0.0 & 0.0 & 0.0 & 106.9 \end{pmatrix},$$

where all necessary and sufficient conditions of $C_{11} > 0$, $C_{11}C_{22} > C_{12}^2$, $C_{44} > 0$, $C_{55} > 0$, $C_{66} > 0$ and $C_{11}C_{22}C_{33} + 2$

$C_{12}C_{13}C_{23} - C_{11}C_{23}^2 - C_{22}C_{13}^2 - C_{33}C_{12}^2 > 0$ are satisfied for elastic stability. In hexagonal Fe_7C_3, the elastic tensor is

$$C = \begin{pmatrix} 342.2 & 174.0 & 154.8 & 0.0 & 0.0 & 0.0 \\ 174.0 & 342.2 & 154.8 & 0.0 & 0.0 & 0.0 \\ 154.8 & 154.8 & 304.7 & 0.0 & 0.0 & 0.0 \\ 0.0 & 0.0 & 0.0 & 89.3 & 0.0 & 0.0 \\ 0.0 & 0.0 & 0.0 & 0.0 & 89.3 & 0.0 \\ 0.0 & 0.0 & 0.0 & 0.0 & 0.0 & 84.1 \end{pmatrix},$$

where all necessary and sufficient conditions of $C_{11} > |C_{12}|$, $2C_{13}^2 < C_{33}(C_{11} + C_{22})$, $C_{44} > 0$ and $C_{66} > 0$ are satisfied for elastic stability. In orthorhombic Fe_7C_3, the elastic tensor is

$$C = \begin{pmatrix} 360.9 & 162.9 & 164.1 & 0.0 & 0.0 & 0.0 \\ 162.9 & 336.0 & 162.4 & 0.0 & 0.0 & 0.0 \\ 164.1 & 162.4 & 346.8 & 0.0 & 0.0 & 0.0 \\ 0.0 & 0.0 & 0.0 & 81.4 & 0.0 & 0.0 \\ 0.0 & 0.0 & 0.0 & 0.0 & 98.3 & 0.0 \\ 0.0 & 0.0 & 0.0 & 0.0 & 0.0 & 65.3 \end{pmatrix},$$

where the necessary and sufficient conditions of $C_{11} > 0$, $C_{11}C_{22} > C_{12}^2$, $C_{44} > 0$, $C_{55} > 0$, $C_{66} > 0$ and $C_{11}C_{22} C_{33} + 2C_{12}C_{13}C_{23} - C_{11}C_{23}^2 - C_{22}C_{13}^2 - C_{33}C_{12}^2 > 0$ are satisfied. So, all the studied compounds are mechanically stable. We also check the spin-polarized phonon dispersion of these compounds, as shown in Fig. 6. All the compounds are dynamically stable. Moreover, we calculated the mechanical properties of bulk modulus and shear modulus for these compounds. The brittle-to-ductile transition is assessed from the ratio of shear-to-bulk modulus, also known as Pugh's ratio. For ductile, Pugh's ratio should be less than 0.571 [44,45]. As listed in Table I, Pugh's ratios in Fe_5C_2, Fe_5SiC, hexagonal and orthorhombic Fe_7C_3 are 0.4, 0.3, 0.4, and 0.4, respectively, thereby implying the ductile behavior.

The theoretical results presented above constitute significant evidence for the feasibility of generating viable permanent-magnet compositions from several Fe-rich ferromagnets with abundant elements. In this section, we take a broader view of this endeavor, by also discussing recent results on the related compounds Fe_5SiB_2 [46] and the alloy system $(\text{Fe}_{1-x}\text{Co}_x)_2\text{B}$ [47]. Permanent magnets, to avoid restrictions on the shapes of manufacture, are often assumed to require a coercivity as large as the magnetization, which in general means that the magnetic hardness parameter κ should be of order unity or greater. Yet recent experimental work [48] on CeCo_5-based "gap magnets" has shown that it is entirely possible to make a viable permanent magnet (with 13 MG Oe energy product) with a coercivity of just half the magnetization and a rather square hysteresis loop, that has in fact already attracted commercial interest [49]. While the magnetic materials considered
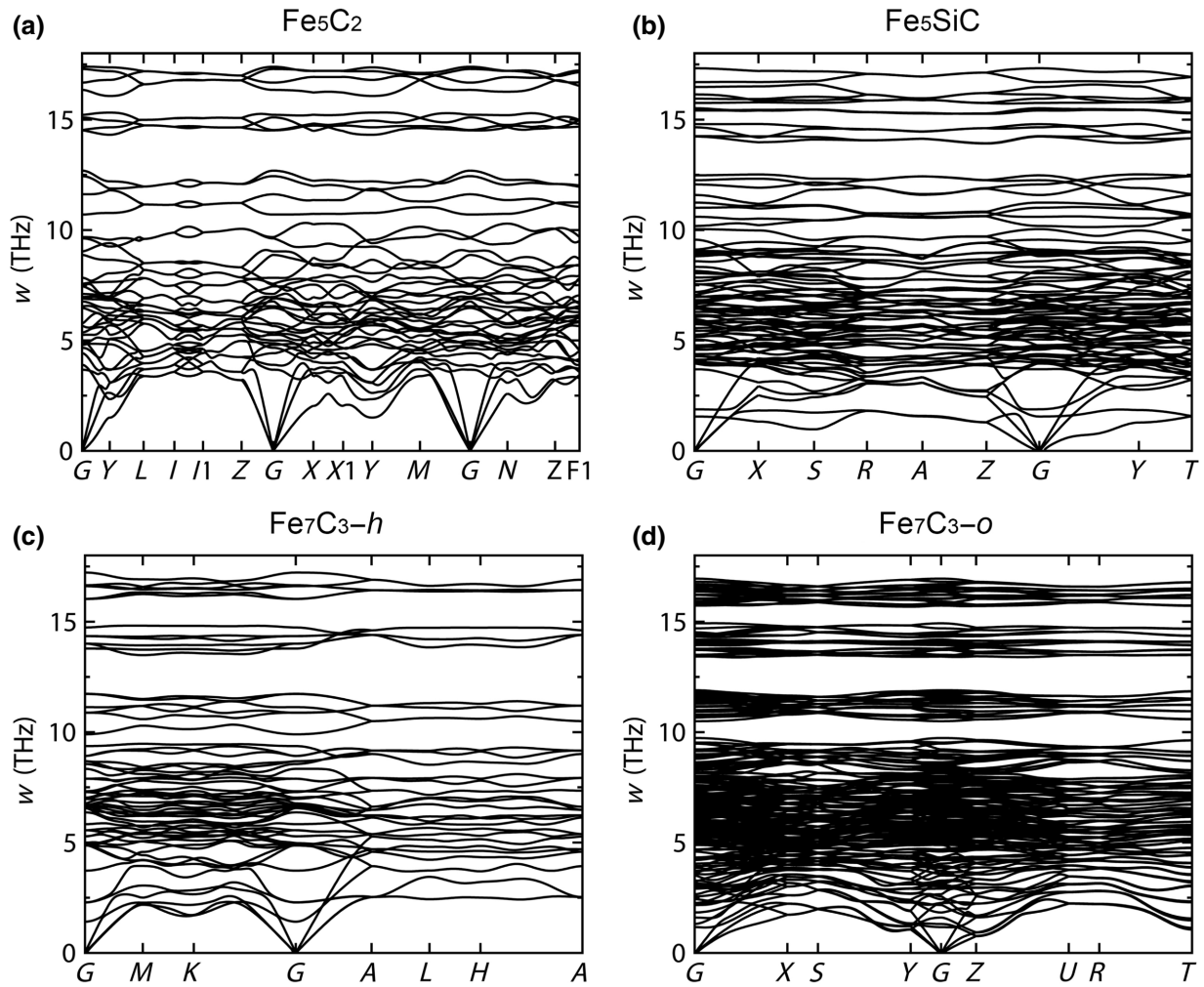
FIG. 6.   Phonon dispersions of (a) Fe_5C_2, (b) Fe_5SiC, (c) hexagonal (-*h*) and (d) orthorhombic (-*o*) Fe_7C_3.

here are not likely to exhibit this level of coercivity, it is well known that the alnico magnet has a κ of approximately 0.5 [50] and yet is in fact a viable commercial magnet. While in alnico this anisotropy arises from shape anisotropy, not magnetocrystalline anisotropy as considered here, the difference matters little for our discussion.

The suggestion is therefore that "semihard" magnetic materials with $\kappa \sim 0.5$ can in fact become highly useful permanent-magnet materials. This effective fourfold reduction in necessary magnetic anisotropy means that there are in fact numerous suitable iron-based magnetic materials. Quantitatively, for a 1-T magnetization, or 796 kA/m, one requires a K_1 of just 0.2 MJ/m^3; for 1.5-T magnetization, the value is 0.45 MJ/m^3. The value for Fe_5SiC described theoretically in this work is in this range. In addition, there are still other iron-based materials, such as Fe_5SiB_2 [46] and $(Fe_{1-x}Co_x)_2B$, $x = 0.3$ [47] with K_1 values in this range; note in addition that Curie points of these materials are favorably high, at respectively 770 and 1030 K.

One may make an estimate of the potential performance of these materials by considering a putative material of 1.5-T magnetization and 0.45 MJ/m^3 K_1, as we in fact find theoretically for Fe_5SiC. For such a material, the anisotropy field H_A is given by the following relationship, where μ_0 is the vacuum permeability:

$$\mu_0 H_A = 2\mu_0 K_1/M_s.$$

From this relationship, one may readily calculate an anisotropy field of 0.75 T for Fe_5SiC. Now, decades of experience in the permanent-magnet community has found that experimentally achievable coercivities can be as large as a quarter, or slightly more, of the anisotropy field, the reduction being related to the "Brown paradox" [51]. On this basis we estimate the achievable coercivity for Fe_5SiC as 0.2 T. The achievable energy product for such a coercivity will depend on the "squareness" of the hysteresis loop. If a fully square loop were to be achieved, given a magnetization of 1.5 T = 15 kG and

coercivity of 0.2 T = 2 kOe, the achieved second-quadrant $BH_{max} = (M - H)H$ would be $(15 - 2) \times 2 = 26$ MG Oe. Note that certain high-performance grades of alnico in fact contain a relatively square hysteresis loop [52], so that even with semihard magnets appreciable coercivity can be achieved.

While 26 MG Oe may be an optimistic figure, the historical experience with $Nd_2Fe_{14}B$ and Sm-Co magnets, where more than 80% of the maximal figure has in fact been achieved, suggests that 20 MG Oe performance in these Fe-based systems is attainable. At the same time, the 1.5-T magnetization in Fe_5SiC is substantially larger than the 1.0–1.2-T magnetization [1,53,54] in alnico 9 magnets, with a comparable κ of 0.45. So we expect that substantially larger BH_{max} should be possible in Fe_5SiC. Note also that high-performance grades of alnico contain as much as 40 wt% of costly cobalt [53]. Given the low materials cost and ready availability of iron and the related elements silicon, carbon, and boron, such a magnet would likely have a substantial technological impact. There is therefore a substantial experimental opportunity to develop inexpensive Fe-based "gap magnets" in this performance range.

V. CONCLUSION

In summary, we study the magnetic properties of iron-carbide and silicocarbide compounds from first principles. All the studied compounds, Fe_5C_2, Fe_5SiC, hexagonal and orthorhombic Fe_7C_3, show the substantial magnetization exceeding 1.4 T and the high Curie point above 520 K. In particular, we find a significant magnetic anisotropy of 0.44 MJ/m^3 and hardness parameter of 0.50 in Fe_5SiC, which is sufficient to make a viable permanent magnet. The significant magnetic anisotropy, strong magnetization, and high Curie point make Fe_5SiC a promising candidate for rare-earth-free and low-cost permanent magnets, especially for room-temperature energy products of 20–25 MG Oe. The recently reported Fe_5SiB_2 and $(Fe_{1-x}Co_x)_2B$ compounds also enrich the Fe-based potential "gap" magnet family. These results provide a foundation for developing Fe-based "gap" permanent magnets with performance in the region between ferrite and Nd-Fe-B (or Sm-Co) magnets.

ACKNOWLEDGEMENTS

---

[1] J. M. D. Coey, Permanent magnets: Plugging the gap, Scr. Mater. **67**, 524 (2012).

[2] J. Mohapatra and J. P. Liu, in *Handbook of Magnetic Materials*, edited by E. Brück (Elsevier, North Holland, 2018), p. 1.

[3] R. W. McCallum, L. H. Lewis, R. Skomski, M. J. Kramer, and I. E. Anderson, Practical aspects of modern and future permanent magnets, Annu. Rev. Mater. Res. **44**, 451 (2014).

[4] A. Athavale, K. Sasaki, B. S. Gagas, T. Kato, and R. D. Lorenz, Variable flux permanent magnet synchronous machine (VF-PMSM) design methodologies to meet electric vehicle traction requirements with reduced losses, IEEE Trans. Ind. Appl. **53**, 4318 (2017).

[5] M. K. D. Manshadi, M. Saadat, M. Mohammadi, R. Kamali, M. Shamsi, M. Naseh, and A. Sanati-Nezhad, Magnetic aerosol drug targeting in lung cancer therapy using permanent magnet, Drug Delivery **26**, 120 (2019).

[6] I. Matsuzaki, M. Hattori, H. Yamauchi, N. Goto, Y. Iwata, T. Yokoi, M. Tsunemi, M. Kobayashi, T. Yamamura, and R. Miyahara, Magnetic anchor-guided endoscopic submucosal dissection for colorectal tumors (with video), Surg. Endosc. **34**, 1012 (2020).

[7] A. Vishina, O. Y. Vekilova, T. Björkman, A. Bergman, H. C. Herper, and O. Eriksson, High-throughput and data-mining approach to predict new rare-earth free permanent magnets, Phys. Rev. B **101**, 094407 (2020).

[8] P. G. Caceres, Low-temperature synthesis of nanostructured $\chi - Fe_5C2$ platelets in $CO + H_2$ atmospheres, Mater. Charact. **56**, 26 (2006).

[9] C. M. Fang, M. H. F. Sluiter, M. A. van Huis, C. K. Ande, and H. W. Zandbergen, Origin of Predominance of Cementite among Iron Carbides in Steel at Elevated Temperature, Phys. Rev. Lett. **105**, 055503 (2010).

[10] P. Spinat and P. Herpin, Etudes par diffraction de neutrons de la phase Mn_5SiC et des solutions solides $(Mn_{1-x}Mo_x)_5SiC$, $(Mn_{1-x}Fe_x)_5SiC$. Propriétés structurales et magnétiques, Bull. Minéral. **99**, 13 (1976).

[11] W. Ge, W. Gao, J. Zhu, and Y. Li, In situ synthesis of Hägg iron carbide (Fe_5C_2) nanoparticles with a high coercivity and saturation magnetization, J. Alloys Compd. **781**, 1069 (2019).

[12] S. Lomayeva, E. P. Elsukov, A. Maratkanova, G. N. Konyigin, and A. V. Zagainov, Structure and magnetic properties of mechanically synthesized iron silicocarbide Fe_5SiC (Russian translation into English, submitted with the paper), Phy. Met. Met. Sci. **99**, 42 (2005).

[13] A. L. Ul'yanov, E. P. Elsukov, M. A. Eremina, A. V. Zagainov, and A. A. Chulkina, Structural and phase transformations during heat treatment of the Fe(71.4)Si(14.3)C(14.3) amorphous alloy prepared by mechanical alloying, Phys. Met. Metallogr. **110**, 542 (2010).

[14] E. P. Yelsukov, A. N. Maratkanova, S. F. Lomayeva, G. N. Konygin, O. M. Nemtsova, A. I. Ul'yanov, and A. A. Chulkina, Structure, phase composition and magnetic properties of mechanically alloyed and annealed quasibinary $Fe(70)Si(x)C(30 − x)$ alloys, J. Alloys Compd. **407**, 98 (2006).

[15] B. Williams, D. Clifford, A. A. El-Gendy, and E. E. Carpenter, Solvothermal synthesis of Fe_7C_3 and Fe_3C nanostructures with phase and morphology control, J. Appl. Phys. **120**, 033904 (2016).

[16] X. Lai, F. Zhu, J. Liu, D. Zhang, Y. Hu, G. J. Finkelstein, P. Dera, and B. Chen, The high-pressure anisotropic thermoelastic properties of a potential inner core carbon-bearing phase, Fe_7C_3, by single-crystal X-ray diffraction, Am. Mineral. **103**, 1568 (2018).

[17] C. Prescher, L. Dubrovinsky, E. Bykova, I. Kupenko, K. Glazyrin, A. Kantor, C. McCammon, M. Mookherjee, Y. Nakajima, N. Miyajima, *et al.*, High Poisson's ratio of Earth's inner core explained by carbon alloying, Nat. Geosci. **8**, 220 (2015).

[18] T. N. Lamichhane, V. Taufour, M. W. Masters, D. S. Parker, U. S. Kaluarachchi, S. Thimmaiah, S. L. Bud'ko, and P. C. Canfield, Discovery of ferromagnetism with large magnetic anisotropy in ZrMnP and HfMnP, Appl. Phys. Lett. **109**, 092402 (2016).

[19] R. Skomski and J. M. D. Coey, Magnetic anisotropy — How much is enough for a permanent magnet?, Scr. Mater. **112**, 3 (2016).

[20] P. Blaha, K. Schwarz, G. K. H. Madsen, D. Kvasnicka, and J. Luitz, *WIEN2k, An Augmented plane wave + local orbitals program for calculating crystal properties* (Technische Universität Wien, Vienna, 2001).

[21] E. Sjöstedt, L. Nordström, and D. J. Singh, An alternative way of linearizing the augmented plane-wave method, Solid State Commun. **114**, 15 (2000).

[22] J. P. Perdew, K. Burke, and M. Ernzerhof, Generalized Gradient Approximation Made Simple, Phys. Rev. Lett. **77**, 3865 (1996).

[23] D. J. Singh and L. Nordstrom, *Planewaves Pseudopotentials and the LAPW Method*, 2nd ed. (Springer, Berlin, 2006).

[24] K. H. Jack and S. Wild, Nature of χ-carbide and its possible occurrence in steels, Nature **212**, 248 (1966).

[25] L. Andreas, S. Shunli, L. Zi-Kui, W. Marc, and N. Rainer, Crystal structure determination of Hägg carbide, $\chi − Fe_5C_2$ by first-principles calculations and rietveld refinement, Z. Kristallogr. **227**, 207 (2012).

[26] F. H. Herbstein and J. A. Snyman, Identification of Eckstrom-Adcock iron carbide as Fe_7C_3, Inorg. Chem. **3**, 894 (1964).

[27] Z. Raza, N. Shulumba, N. M. Caffrey, L. Dubrovinsky, and I. A. Abrikosov, First-principles calculations of properties of orthorhombic iron carbide Fe_7C_3 at the Earth's core conditions, Phys. Rev. B **91**, 214112 (2015).

[28] G. Kresse and J. Furthmüller, Efficient iterative schemes for ab initio total-energy calculations using a plane-wave basis set, Phys. Rev. B **54**, 11169 (1996).

[29] G. Kresse and J. Furthmüller, Efficiency of ab-initio total energy calculations for metals and semiconductors using a plane-wave basis set, Comput. Mater. Sci. **6**, 15 (1996).

[30] G. Kresse and D. Joubert, From ultrasoft pseudopotentials to the projector augmented-wave method, Phys. Rev. B **59**, 1758 (1999).

[31] P. E. Blöchl, Projector augmented-wave method, Phys. Rev. B **50**, 17953 (1994).

[32] E. K. Delczeg-Czirjak, A. Edström, M. Werwiński, J. Rusz, N. V. Skorodumova, L. Vitos, and O. Eriksson, Stabilization of the tetragonal distortion of $Fe_xCo_{1−x}$ alloys by C impurities: A potential new permanent magnet, Phys. Rev. B **89**, 144403 (2014).

[33] L. Reichel, G. Giannopoulos, S. Kauffmann-Weiss, M. Hoffmann, D. Pohl, A. Edström, S. Oswald, D. Niarchos, J. Rusz, L. Schultz, *et al.*, Increased magnetocrystalline anisotropy in epitaxial Fe-Co-C thin films with spontaneous strain, J. Appl. Phys. **116**, 213901 (2014).

[34] J. Thakur, P. Rani, M. Tomar, V. Gupta, H. S. Saini, and M. K. Kashyap, Tailoring in-plane magnetocrystalline anisotropy of Fe_5SiB_2 with Cr-substitution, AIP Conf. Proc. **2115**, 030506 (2019).

[35] G. Rahman and H. U. Jan, Elastic and magnetic properties of cubic Fe_4C from first-principles, J. Supercond. Novel Magn. **31**, 405 (2018).

[36] J. Cui, M. Kramer, L. Zhou, F. Liu, A. Gabay, G. Hadjipanayis, B. Balasubramanian, and D. Sellmyer, Current progress and future challenges in rare-earth-free permanent magnets, Acta Mater. **158**, 118 (2018).

[37] J. Brandenburg, R. Hühne, L. Schultz, and V. Neu, Domain structure of epitaxial Co films with perpendicular anisotropy, Phys. Rev. B **79**, 054429 (2009).

[38] W. Tang, Z. Zhen, C. Yang, L. Wang, T. Cowger, H. Chen, T. Todd, K. Hekmatyar, Q. Zhao, Y. Hou, *et al.*, Fe_5c_2 nanoparticles with high MRI contrast enhancement for tumor imaging, Small **10**, 1245 (2014).

[39] T. Hamaya, J. Oikawa, M. Doi, and H. Asano, Magnetic properties of Fe_3C thin film prepared by the IBS method, Trans. Magn. Soc. Japan **2**, 59 (2002).

[40] J. Liu, J. Li, and D. Ikuta, Elastic softening in Fe_7C_3 with implications for Earth's deep carbon reservoirs, J. Geophys. Res. Solid Earth **121**, 1514 (2016).

[41] A. Tsuzuki, S. Sago, S. I. Hirano, and S. Naka, High temperature and pressure preparation and properties of iron carbides Fe_7C_3 and Fe_3C, J. Mater. Sci. **19**, 2513 (1984).

[42] A. Jain, S. P. Ong, G. Hautier, W. Chen, W. D. Richards, S. Dacek, S. Cholia, D. Gunter, D. Skinner, G. Ceder, *et al.*, Commentary: The materials project: A materials genome approach to accelerating materials innovation, APL Mater. **1**, 011002 (2013).

[43] F. Mouhat and F.-X. Coudert, Necessary and sufficient elastic stability conditions in various crystal systems, Phys. Rev. B **90**, 224104 (2014).

[44] V. Kanchana, G. Vaitheeswaran, X. Zhang, Y. Ma, A. Svane, and O. Eriksson, Lattice dynamics and elastic properties of the $4f$ electron system: CeN, Phys. Rev. B **84,** 205135 (2011).

[45] S. F. Pugh, XCII. relations between the elastic moduli and the plastic properties of polycrystalline pure metals, Philos. Mag. **45,** 823 (1954).

[46] M. A. McGuire and D. S. Parker, Magnetic and structural properties of ferromagnetic Fe_5PB_2 and Fe_5SiB_2 and effects of Co and Mn substitutions, J. Appl. Phys. **118,** 163903 (2015).

[47] T. N. Lamichhane, O. Palasyuk, P. Antropov, I. A. Zhuravlev, K. D. Belashchenko, I. C. Nlebedim, K. W. Dennis, A. Jesche, M. J. Kramer, S. L. Budko, *et al.*, Reinvestigation of the intrinsic magnetic properties of $(Fe_{1-x}Co_x)_2B$ alloys and crystallization behavior of ribbons, J. Magn. Magn. Mater. **513,** 167214 (2020).

[48] T. N. Lamichhane, M. T. Onyszczak, O. Palasyuk, S. Sharikadze, T.-H. Kim, Q. Lin, M. J. Kramer, R. W. McCallum, A. L. Wysocki, M. C. Nguyen, *et al.*, Single-crystal Permanent Magnets: Extraordinary Magnetic Behavior in the Ta-, Cu-, and Fe-Substituted $CeCo_5$ Systems, Phys. Rev. Appl. **11,** 014052 (2019).

[49] A. Palasyuk, Personal communication (2020).

[50] J. M. D. Coey, Perspective and prospects for rare earth permanent magnets, Engineering **6,** 119 (2020).

[51] D. Goll and H. Kronmüller, High-performance permanent magnets, Naturwissenschaften **87,** 423 (2000).

[52] Catalog of Arnold Magnetics cast Alnico products. Available at https://www.arnoldmagnetics.com/wp-content/uploads/2017/10/Cast-Alnico-Permanent-Magnet-Brochure-101117-1.pdf; see especially performance characteristics for Alnico 9 on p. 6.7.

[53] T. Liu, W. Li, M. Zhu, Z. Guo, and Y. Li, Effect of Co on the thermal stability and magnetic properties of AlNiCo 8 alloys, J. Appl. Phys. **115,** 17A751 (2014).

[54] Q. Gao, I. Opahle, O. Gutfleisch, and H. Zhang, Designing rare-earth free permanent magnets in heusler alloys via interstitial doping, Acta Mater. **186,** 355 (2020).

[55] DOE Public Access Plan, http://energy.gov/downloads/doe-public-access-plan.